Supplementary Material

Hierarchical bionic neural network-like architecture towards high-performance microwave absorption and corrosion protection

Shuaizhen Li [1, 2], Tianwen Xie [1, 2], Lin Ma [1, 2], Daheng Liu [1, 2], Nan Huang [1], Wei Liu [1], Song Ma [1, *] and Zhidong Zhang [1]

[1] Shenyang National Laboratory for Materials Science, Institute of Metal Research, Chinese Academy of Sciences 72 Wenhua Road, Shenyang 110016, China

[2] School of Materials Science and Engineering, University of Science and Technology of China, 72 Wenhua Road, Shenyang 110016, China

**Song Ma. E-mail: songma@imr.ac.cn*

Fig. S1

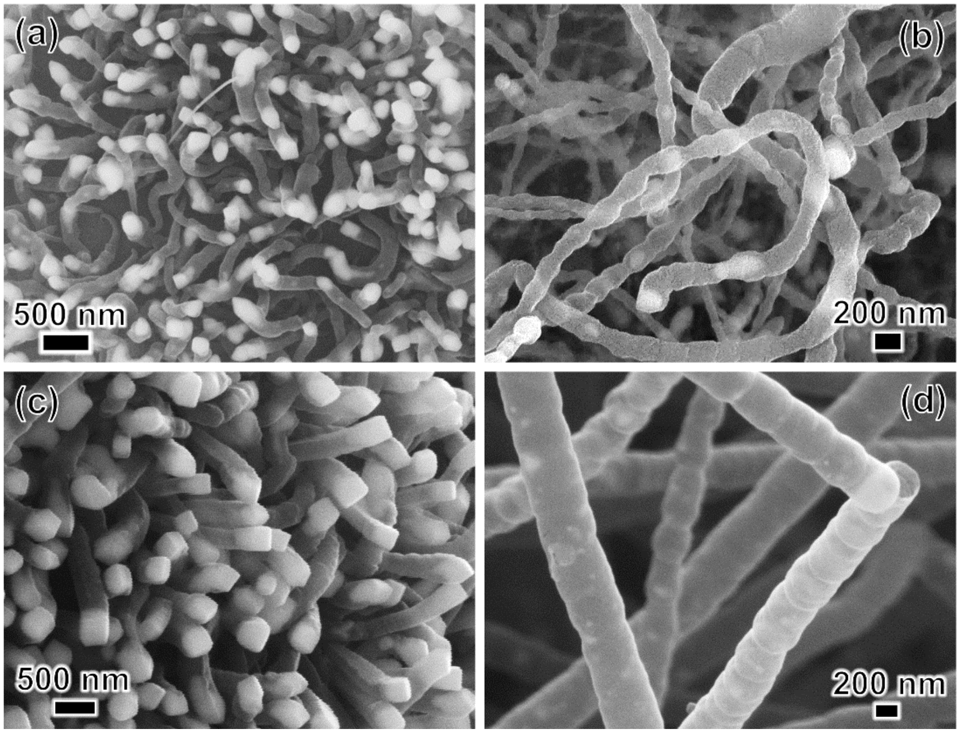

Fig. S1 SEM images of **a** short CNTs and **b** long CNTs of NNCF-1; **c** short CNTs and **d** long CNTs of NNCF-3

Fig. S2

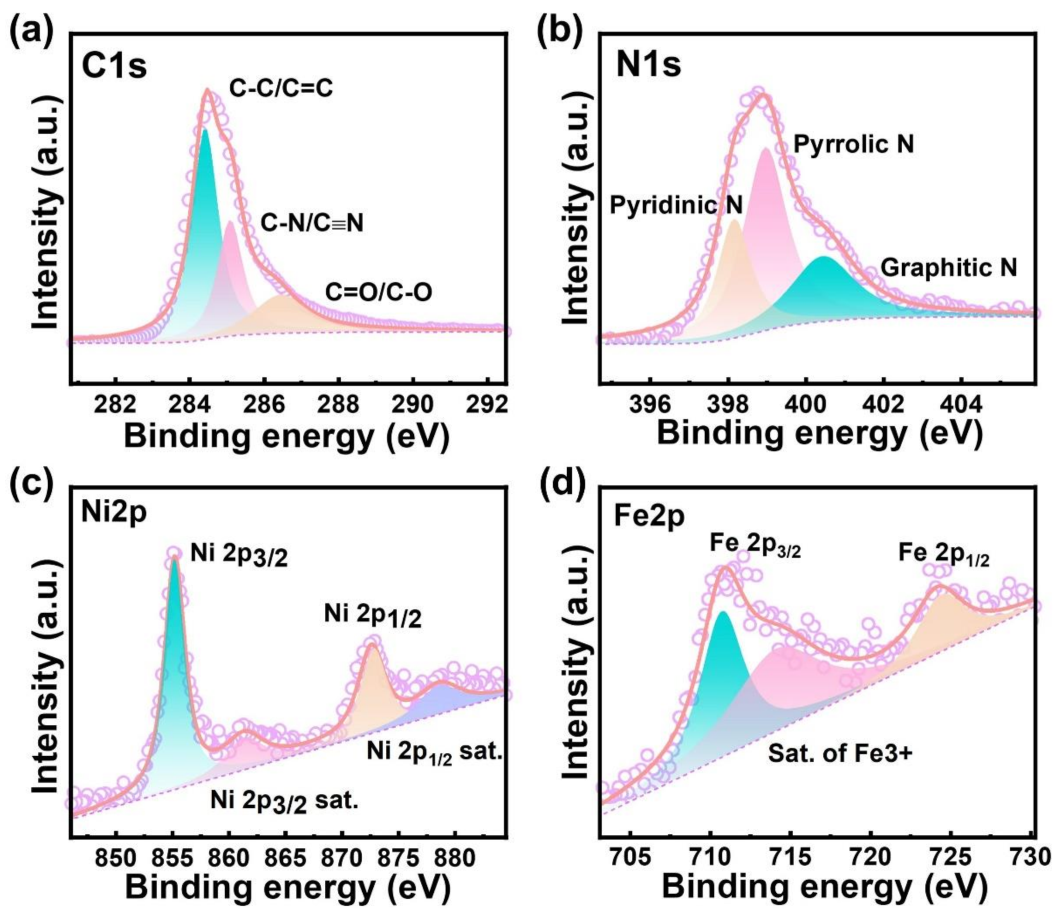

Fig. S2 XPS spectra of **a** C1s; **b** N1s; **c** Ni2p and **d** Fe2p of NNCF-2 composite

Fig. S3

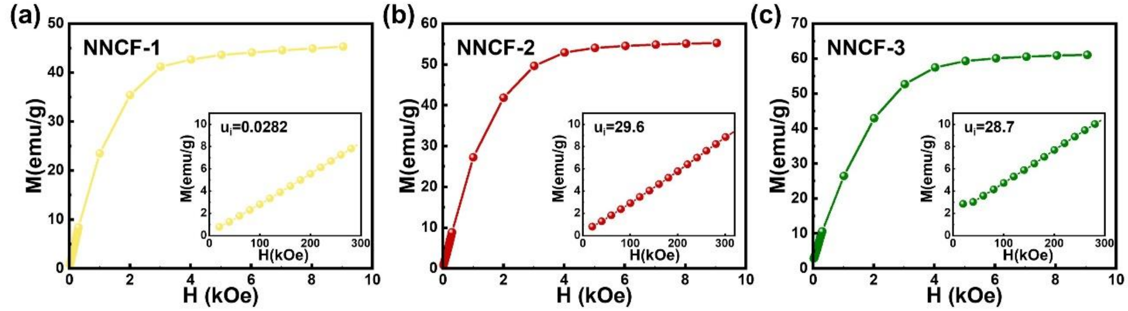

Fig. S3 The initial permeability of **a** NNCF-1; **b** NNCF-2; **c** NNCF-3

Fig. S4

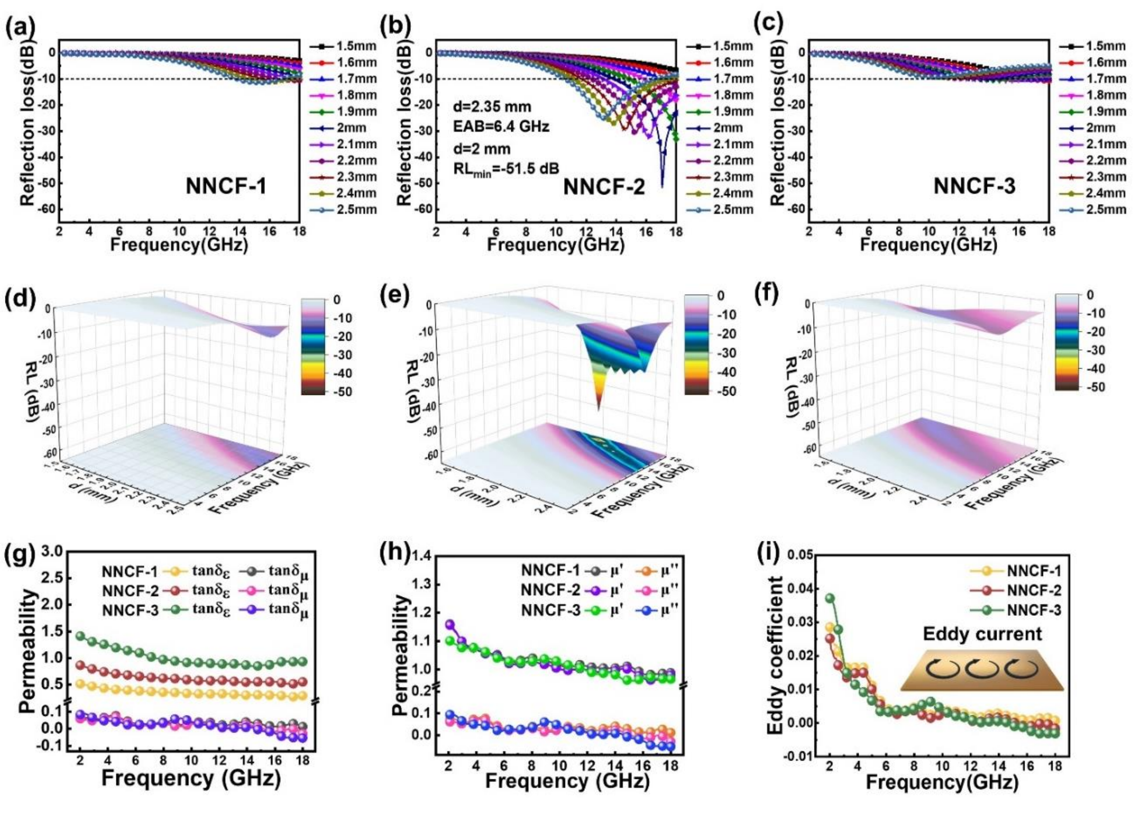

Fig. S4 Dependence of RL values on the thickness of **a, d** NNCF-1; **b, e** NNCF-2 and **c, f** NNCF-3 with the filling ratio 10 wt% during 2-18 GHz; **g** dielectric and magnetic loss angle tangent of three samples; **h** the real and imaginary parts of the permeability of NNCF-1, NNCF-2 and NNCF-3; **i** eddy coefficient C_0 value of NNCF-1, NNCF-2 and NNCF-3

Therein, RL values ware characterized by equations based on transmission line theory according to openly announced research [1].

$$\mathrm{RL} = 20\lg\frac{|Z_{in}-Z_0|}{|Z_{in}+Z_0|} \tag{1}$$

$$Z_0 = \sqrt{\frac{\mu_0}{\varepsilon_0}} \tag{2}$$

$$Z_{in} = Z_0\sqrt{\frac{\mu_r}{\varepsilon_r}}\tanh\left[j\left(\frac{2\pi f d}{c}\right)\sqrt{\mu_r\varepsilon_r}\right] \tag{3}$$

where Z_0 is the characteristic impedance of free space, Z_{in} is the normalized input impedance of a metal-backed microwave absorbing layer, μ_0 and ε_0 is the permeability and the dielectric constant of free space, respectively, ε_r and μ_r is the measured relative permittivity ($\varepsilon_r = \varepsilon' - j\varepsilon''$) and permeability ($\mu_r = \mu' - j\mu''$), respectively, f is the frequency, c is the velocity of light, d is the thickness.

Besides, α is related to the EMW energy assimilated by the absorber and impedance matching Δ is associated with the degree that EMW propagates the inside of the absorber, which are evaluated by the following formulas [2]:

$$\alpha=\frac{\sqrt{2}\pi f}{c}\sqrt{(\mu''\varepsilon''-\mu'\varepsilon')+\sqrt{(\mu''\varepsilon''-\mu'\varepsilon')^2+(\mu'\varepsilon''-\mu''\varepsilon')^2}} \tag{4}$$

$$\Delta=\left|\sinh^2(kfd)-M\right| \tag{5}$$

$$K=\frac{4\pi}{c}\sqrt{\varepsilon'\mu'}\,\frac{\sin\left(\frac{\delta_\varepsilon+\delta_\mu}{2}\right)}{\sqrt{\cos(\delta_\varepsilon)\cos(\delta_\mu)}} \tag{6}$$

$$M=\frac{4\varepsilon'\cos(\delta_\varepsilon)\mu'\cos(\delta_\mu)}{(\mu'\cos(\delta_\varepsilon)-\varepsilon'\cos(\delta_\mu))^2\left(1+\tan^2\left(\frac{\delta_\mu-\delta_\varepsilon}{2}\right)\right)} \tag{7}$$

where δ_ε=arctan ($\varepsilon''/\varepsilon'$) and δ_μ= arctan (μ''/μ') are the dielectric loss and magnetic loss angle, respectively.

Fig. S5

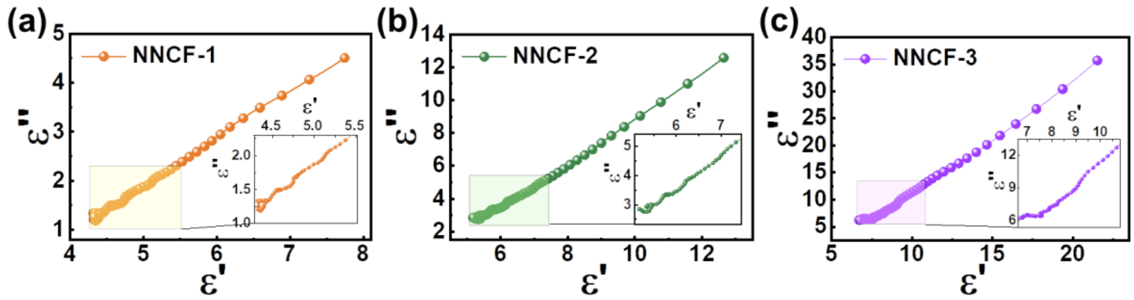

Fig. S5 Cole-Cole plots of **a** NNCF-1; **b** NNCF-2 and **c** NNCF-3 (The three insets are the local magnification of Cole-Cole semicircles in the high-frequency band for each sample, respectively)

Fig. S6

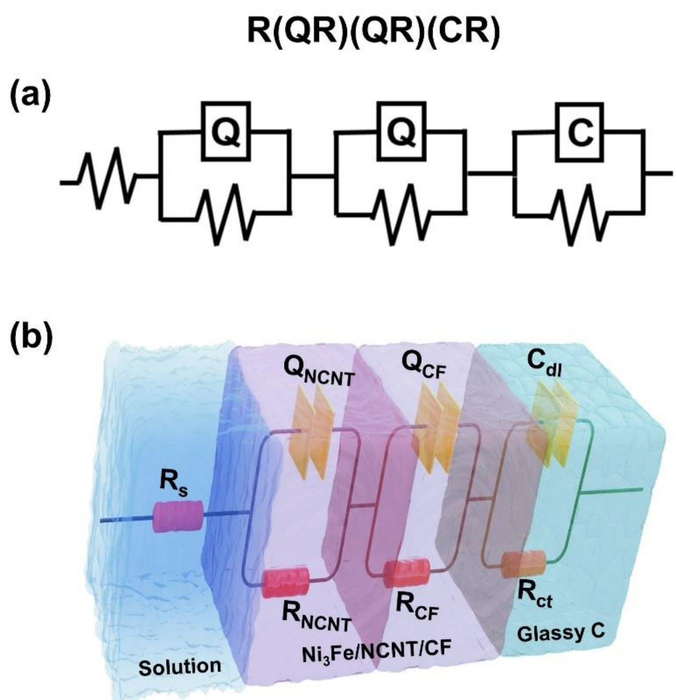

Fig. S6 Equivalent circuit of **a, b** NNCF-2 coating soaked in neutral 3.5wt% NaCl test environments for 720 hours (Here the circuit model is R(QR)(QR)(CR))

Fig. S7

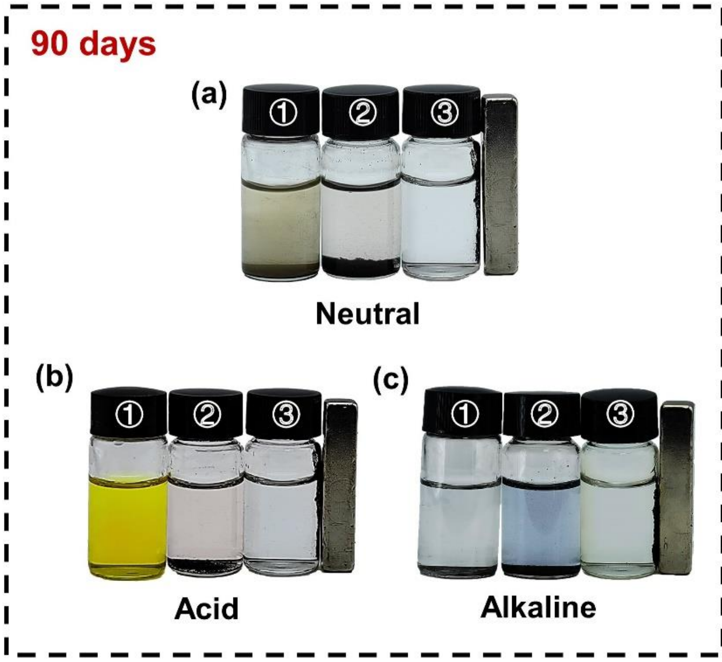

Fig. S7 NNCF-2 (right), together with CIP (left) and Co-MOF derivative (middle) immersed in three corrosive NaCl environments. **a** neutral; **b** acid; **c** alkaline. By contrast, NNCF-2 shows the most satisfactory corrosion resistance, comprehensively.

Table S1 Comparison of EMW absorbing performances of related advanced CF or CNT incorporated microwave absorbents (MAMs)

Absorbents	**Filler loading** [wt%]	**Maximum RL** [dB][a)]	**Thickness** [mm]	**EAB** [GHz][b)]	**Refs**
CF/Ni	25	-45	2	5.1	[2]
CF/Fe_3O_4	30	-26.45	5	4.28	[3]
CF/CuNi	40	-50.2	1.6	2.5	[4]
Fe_3O_4@$Ti_3C_2T_x$/CNTs	20	-40.1	2	5.8	[5]
CF/CoNi@C	20	-60	1.6	6.07	[6]
CF/Co@C	20	-59.82	2.3	5.64	[7]
CF/Co	30	-46.2	2	4.8	[8]
CF/CNTs/Fe_3C/Fe_3O_4	20	-40.47	2.11	6.0	[9]
CF/Ni/CNT	30	-47.0	1.8	5.8	[10]
CF/$NiCo_2O_4$	40	-63.6	2.8	4.72	[11]
CoNi@G@NCNTs	55	-54	2.5	5.2	[12]
Co@NCNT	25	-53.0	1.8	6.2	[13]
Co_1Zn_1@HNCNTS	20	-44.2	1.7	4.8	[14]
MWCNT/Ni	60	-37.0	5.2	2.1	[15]
MWCNT/Fe	60	-39.0	4.3	2.7	[15]
MWCNT/Co	60	-37.0	5.3	2.8	[15]
CMT@CNT/Co	15	-52.2	2	5.1	[16]
Ni/SnO_2/MWCNT	75	-39.2	1.5	3.6	[17]
Fe_3O_4/ PPy/CNT	20	-25.9	3	4.5	[18]
FeNi@CNT/CNRs	20	-47	2.3	4.5	[19]
CoNi@NCNT	10	-55.62	1.45	4.25	[20]
$NiCo_2$/CNT	50	-25.5	1.3	4.4	[21]
CF/Ni_3Fe/NCNT	10	-51.5	2.35	6.4	herein

[a)] Maximum value of reflection loss; [b)] Effective absorption bandwidth

Table S2 Corrosion kinetic parameters of NNCF-2, CIP and Co/C coatings immersed in neutral 3.5 wt% NaCl solution for 720 hours, respectively

Sample	E_{corr} [V]	I_{corr} [A cm^{-2}]	β_a [mV]	β_c [mV]	R_p [Ω]
NNCF-2	0.03118	2.79E-08	86.53	-89.206	2.54E+07
CIP	-0.054788	3.28E-07	318.8	-76.362	7.83E+04
Co/C	-0.14277	2.26E-07	117.49	-116.27	1.17E+05

$$R_P = \frac{\beta_a \beta_c}{I_{corr} \ln(10)(\beta_a + \beta_c)}$$

Here, β_a and β_c are on behalf of the slopes of anodic and cathodic Tafel plots, respectively. It can be concluded from Table S2 that the value of I_{corr} is in the following order: $I_{corr\text{-}NNCF\text{-}2} < I_{corr\text{-}CIP} < I_{corr\text{-}Co/C}$, for R_p, $R_{p\text{-}NNCF\text{-}2}$ is the largest and $R_{p\text{-}CIP}$ is the smallest. In general, I_{corr} and R_p can be used as parameters for qualitatively judging the anti-corrosion property of the coating, [22] the smaller the value of I_{corr}, the better anti-corrosion property of the coating while for R_p, the smaller, the worse. Hence, it can be preliminarily confirmed that the anti-corrosion property of the NNCF-2 coating was the most favorable.

Table S3 Equivalent circuit parameters of the NNCF-2 coating with the passage of soaking time in the neutral 3.5 wt% NaCl environment

R(QR)(QR)(CR)

NNCF-2	3h	24h	168h	360h	720h
R_s [Ω cm^2]	51.18	42.98	34.19	31.34	30.26
CPE_{NCNT} [F cm^{-2}]	5.652E-5	6.638E-5	1.274E-4	7.657E-5	1.298E-4
n	0.7868	0.8203	0.6119	0.8299	0.8108
R_{NCNT} [Ω cm^2]	1075	1164	1048	986.4	900.6
CPE_{CF} [F cm^{-2}]	2.063E-4	1.16E-4	7.133E-5	3.282E-4	1.289E-4
n	0.4878	0.5994	0.8159	0.6295	0.7201
R_{CF} [Ω cm^2]	450.2	374.4	354.2	323.1	260.5
C_{dl} [F cm^{-2}]	2.928E-5	1.094E-5	1.034E-4	1.622E-4	1.207E-4
R_{ct} [Ω cm^2]	8.542E5	7.786E5	7.345E5	7.042E5	6.965E5

References

1. Wang FY, Liu YL, Zhao HH, Cui LR, Gai LX, Han XJ, Du YC (2022) Controllable seeding of nitrogen-doped carbon nanotubes on three-dimensional Co/C foam for enhanced dielectric loss and microwave absorption characteristics. Chem. Eng. J. 450： 138160. https://doi.org/10.1016/j.cej.2022.138160

2. Sun QY, Shi JY, Wu LP, Wu F, Xie AM (2021) Ni@Carbon nanocomposites with hierarchical three-dimensional network for electromagnetic waves absorption. Ceram. Int. 47:27577–27585. https://doi.org/10.1016/j.ceramint.2021.06.182

3. Jiang S, Qian K, Yu KJ, Zhou HF, Weng YX, Zhang ZW (2021) Study on ultralight and flexible Fe_3O_4/melamine derived carbon foam composites for high-efficiency microwave absorption. Chem. Phys. Lett. 779:138873. https://doi.org/10.1016/j.cplett.2021.138873

4. Lu LF, Wang FL, Zhang X, Qiao J, Liu C,Liu JR (2021) CuNi alloy/ carbon foam nanohybrids as high-performance electromagnetic wave absorbers. Carbon 172: 488-496. https://doi.org/10.1016/j.carbon.2020.10.021

5. Zhang C, Wu ZC, Xu CY, Yang BT, Wang L, You WB, and Che RC (2022) Hierarchical $Ti_3C_2T_x$ MXene/carbon nanotubes hollow microsphere with confined magnetic nanospheres for broadband microwave absorption. Small 18:2104380. https://doi.org/10.1002/smll.202104380

6. Wang MQ, Wei B, Zhou JT, Yao ZJ, Xu LL, Zhang XF, Tao JQ, Shi ZJ (2022) Multi-scale CoNi nano-alloy/CoNi@C microsphere/3D macropores N-doped carbon foam composites: Lightweight and efficient electromagnetic wave absorption characteristics. Mater. Chem. Phys. 279:125777.

https://doi.org/10.1016/j.matchemphys.2022.125777

7. Gu WH, Tan JW, Chen JB, Zhang Z, Zhao Y, Yu JW, Ji GB (2020) Multifunctional bulk hybrid foam for infrared stealth, thermal insulation, and microwave absorption. ACS Appl. Mater. Interfaces 12:28727−28737. https://doi.org/10.1021/acsami.0c09202

8. Shi HG, Wang T, Cheng JB, Zhao HB, Li SL, Wang YZ (2021) Ultralow-density carbon foam composites with bean-like Co-embedded carbon nanotube whiskers towards high-performance microwave absorption. J. Alloys Compd. 863:158090. https://doi.org/10.1016/j.jallcom.2020.158090

9. Jia TM, Qi XS, Wang L, Yang JL, Gong X, Chen YL, Qu YP, Peng Q, Zhong W (2023) Constructing mixed-dimensional lightweight flexible carbon foam/carbon nanotubes-based heterostructures: An effective strategy to achieve tunable and boosted microwave absorption. Carbon 206:364–374. https://doi.org/10.1016/j.carbon.2023.02.046

10. Liu DW, Yang L, Wang FY, Zhang H, Liu J, Lv T, Zhao HJ, Du YC (2022) Hierarchical carbon nanotubes@Ni/C foams for high-performance microwave absorption. Carbon 196:867–876. https://doi.org/10.1016/j.carbon.2022.05.057

11. Zheng SN, Lyu LF, Wang FL, Liu Y, Liu JR (2021) Self-supported construction of three-dimensional $NiCo_2O_4$ hierarchical nanoneedles for high-performance microwave absorption. Ceram. Int. 47:34289–34296. https://doi.org/10.1016/j.ceramint.2021.08.339

12. Guo D, Yuan HR, Wang XC, Zhu CL, Chen YJ (2020) Urchin-like amorphous nitrogen-doped carbon nanotubes encapsulated with

transition-metal-alloy@graphene core@shell nanoparticles for microwave energy attenuation. ACS Appl. Mater. Interfaces 12:9628–9636. https://doi.org/10.1021/acsami.9b20412

13. Huang MQ, Wang L, Pei K, You WB, Yu XF, Wu ZC, Che RC (2020) Multidimension-controllable synthesis of MOF-derived Co@N-Doped carbon composite with magnetic-dielectric synergy toward strong microwave absorption. Small 16:2000158. https://doi.org/10.1002/smll.202000158

14. Li KY, Sun H, Zhang X, Zhang S, Dong HW, Zhu CL, Chen YJ (2020) Micro-nanospheres assembled with helically coiled nitrogen-doped carbon nanotubes: Fabrication and microwave absorption properties. Mater. Des. 186 108290. https://doi.org/10.1016/j.matdes.2019.108290

15. Wen FS, Zhang F, Liu ZY (2011) Investigation on microwave absorption properties for multiwalled carbon nanotubes/Fe/Co/Ni nanopowders as lightweight absorbers. J. Phys. Chem. C 115:14025–14030. https://doi.org/10.1021/jp202078p

16. Wu ZC, Pei K, Xing LS, Yu XF, You WB, Che RC (2019) Enhanced microwave absorption performance from magnetic coupling of magnetic nanoparticles suspended within hierarchically tubular composite. Adv. Funct. Mater. 29: 1901448. https://doi.org/10.1002/adfm.201901448

17. Lin L, Xing HL, Shu RW, Wang L, Ji XL, Tan DX, Gan Y (2015) Preparation and microwave absorption properties of multi-walled carbon nanotubes decorated with Ni-doped SnO_2 nanocrystals. RSC Adv. 5:94539-94550. https://doi.org/10.1039/C5RA17303E

18. Yang R-B, Reddy PM, Chang C-J, Chen P-A, Chen J-K, Chang C-C (2016) Synthesis

and characterization of Fe_3O_4/polypyrrole/carbon nanotube composites with tunable microwave absorption properties: Role of carbon nanotube and polypyrrole content. Chem. Eng. J. 285:497-507. https://doi.org/10.1016/j.cej.2015.10.031

19. Xu XQ, Ran FT, Lai H, Cheng ZJ, Lv T, Shao L, Liu YY (2019) In situ confined bimetallic metal–organic framework derived nanostructure within 3D interconnected bamboo-like carbon nanotube networks for boosting electromagnetic wave absorbing performances. ACS Appl. Mater. Interfaces 11:35999–36009. https://doi.org/10.1021/acsami.9b14754

20. L-L Liang, Z Liu, L-J Xie, J-P Chen, H Jia, Q-Q Kong, G-H Sun, C-M Chen (2021) Bamboo-like N-doped carbon tubes encapsulated CoNi nanospheres towards efficient and anticorrosive microwave absorbents. Carbon 171:142-153. https://doi.org/10.1016/j.carbon.2020.08.057

21. Wang BC, Zhang C, Mu CP, Yang RL, Xiang JY, Song JF, Wen FS, Liu ZY (2019) Enhanced electromagnetic wave absorption properties of $NiCo_2$ nanoparticles interspersed with carbon nanotubes. J. Magn. Magn. Mater. 471:185-191. https://doi.org/10.1016/j.jmmm.2018.09.090

22. D Prasai, JC Tuberquia, RR Harl, GK Jennings, KI Bolotin (2012) Graphene: Corrosion-inhibiting coating. ACS Nano 6:1102–1108. https://doi.org/10.1021/nn203507y